Plasticity of the dopaminergic phenotype and of locomotion in larval zebrafish induced by changes in brain excitability during the embryonic period

Sandrine Bataille, Hadrien Jalaber, Ingrid Colin, Damien Remy, Pierre Affaticati, Cynthia Froc, Philippe Vernier, Michaël Demarque

⁛ *Title (50 w)*

Plasticity of the dopaminergic phenotype and of locomotion in larval zebrafish induced by changes in brain excitability during the embryonic period.

Embryonic excitability modulates differentiation

Sandrine Bataille*[1], Hadrien Jalaber*[1], Ingrid Colin*[1], Damien Remy[1], Pierre Affaticati[2], Cynthia Froc[1], Philippe Vernier[1] and Michaël Demarque**[1].

1. Paris Saclay Institute of Neuroscience, (UMR9197) CNRS and Université Paris-Saclay; Avenue de la Terrasse, 91190 Gif-sur-Yvette, France

2. TEFOR Paris-Saclay, CNRS UMS2010 / INRAE UMS1451, Université Paris-Saclay, Avenue de la Terrasse, 91190 Gif-sur-Yvette, France

*authors contributed equally

**Corresponding author

⁛ *Corresponding author email address: michael.demarque@cnrs.fr*

⁛ *Number of pages: 39*

⁛ *Number of figures, tables, multimedia, and 3D models (separately): 6/0/0/0*

⁛ *Number of words for abstract, introduction, and discussion: 233/646/1261*

⁛ *Conflict of interest statement:* The authors declare no competing financial interests.

⁛ *Acknowledgments:* This work was funded by the French National Research Agency (ANR project “PallEnody”) and the Fondation pour la Médicale Recherche, FRM (“team FRM”). The authors thank Kei Yamamoto for scientific inputs, TEFOR Paris Saclay (TPS) for technical support.

ABSTRACT (233/250 w):

During the embryonic period, neuronal communication starts before the establishment of the synapses with forms of neuronal excitability, called here Embryonic Neuronal Excitability (ENE). ENE has been shown to modulate the correct unfolding of development transcriptional programs but the global consequences for the developing organisms are not all understood. Here we monitored calcium transients in zebrafish embryos as a proxy for ENE to assess the efficacy of transient pharmacological treatments able to either increase or decrease ENE. Increasing or decreasing ENE for 24 hour at 2 days post fertilization (dpf) promoted respectively an increase or decrease in the post-mitotic differentiation of the dopamine (DA) neurons in the telencephalon and in the olfactory bulb of zebrafish larvæ at 6 dpf. This plasticity of dopaminergic specification occurs within a stable population of vMAT2 immuno-reactive cells, hence identifying an unanticipated biological marker for this pool of reserve cells, that can be recruited through ENE.

Modulating ENE also affected locomotion several days after the end of the treatments. In particular, the increase of ENE from 2 to 3 dpf promoted an hyperlocomotion in 6 dpf zebrafish larvæ, reminiscent of endophenotypes reported for Attention Deficit with Hyperactivity Disorders and schizophrenia in zebrafish. These results provide a convenient framework to identify environmental factors that could disturb ENE as well as to study the molecular mechanisms linking ENE to the neurotransmitters specification, with clinical relevance for the pathogenesis of neurodevelopmental disorders.

Significance Statement (109/ 120 w):

- Spontaneous calcium spikes, used as a proxy for Embryonic Neuronal Excitability (ENE), are detected in the forebrain of embryonic zebrafish.
- Transients pharmacological treatments applied by balneation could be used to increase or decrease ENE.
- The post-mitotic differentiation of the dopaminergic phenotype is modulated by ENE in the zebrafish forebrain.
- The plasticity of the dopaminergic specification occurs within a reserve pool of vMAT2 immuno-reactive cells.
- Transient increase of ENE at the end of the embryonic period induces a hyperlocomotion, a phenotype associated with ADHD and schizophrenia in this model.
- Our results open clinically relevant perspectives to study the pathogenesis of neurodevelopmental disorders in zebrafish.

Introduction (646/650 w)

During brain development, specific molecular components of the synaptic neuronal communication such as ion channels, neurotransmitters and neurotransmitter receptors are expressed and functional before synapse formation (Spitzer et al., 2002). They contribute to immature forms of cellular excitability and intercellular communications we propose to refer to as Embryonic Neuronal Excitability (ENE). There is for instance a paracrine communication mediated by activation of receptors by endogenous neurotransmitters, GABA and glutamate, in the neonatal rat hippocampus, or glycine in the mouse spinal cord (Demarque et al., 2002; Owens & Kriegstein, 2002; Scain et al., 2010). Acute changes of calcium concentration have also been described, including filopodial or growth cone transients, and calcium spikes

in differentiating neurons (Gomez & Spitzer, 1999; Gomez et al., 2001; Borodinsky et al., 2004). Calcium spikes are sporadic, long lasting global increase of intracellular concentration of Ca^{2+} that occurs during restricted developmental windows called "critical periods". They have been identified in the developing brain of several vertebrate species (Owens & Kriegstein, 1998; Borodinsky et al., 2004; Crepel et al., 2007; Blankenship & Feller, 2010; Demarque & Spitzer, 2010; Warp et al., 2012; Plazas et al., 2013). Quantification of calcium spikes by calcium imaging can be used as proxy for ENE. Changes in the incidence and frequency of calcium spikes modulate the specification of the neurotransmitter phenotype in neurons, as it is the case for dopamine (DA), in several cell populations of the xenopus and mouse brain, with consequences on several behaviors (Dulcis & Spitzer, 2008; Dulcis et al., 2013, 2017).

DA is an evolutionary conserved monoamine involved in the neuromodulation of numerous brain functions in vertebrates, including motivational processes, executive functions and motor control (Klein et al., 2019). Accordingly, alterations of the differentiation and function of the neurons synthetizing DA contribute to the pathogenesis of several brain disease with a neurodevelopmental origin, such as Attention Deficit Hyperactivity Disorder (ADHD) and schizophrenia (SZ) (Lange et al., 2012; Murray et al., 2017).

Further addressing the complex molecular and cellular mechanisms linking developmental excitability, dopaminergic differentiation and behavioral outputs requires an *in vivo* approach in a model accessible, genetically amenable and with possible parallels with the human situations. The developing zebrafish *Brachydanio rerio* fits with these needs. The development of the embryos is external, which allows inducing perturbations of ENE at stages that would be *in utero* in mammalian models. The embryos are relatively small and transparent, simplifying high-resolution imaging

of the brain in live or fixed preparations. Despite difference in the brain organization, notably a pallium very different form the 6-layered cortex of mammals, the main neuronal systems of vertebrates are present in zebrafish and respond to psychoactive drugs (Gawel et al., 2019). In addition, the monoaminergic system has been extensively studied in zebrafish (Schweitzer & Driever, 2009; Schweitzer et al., 2012). In vertebrates, DA modulates executive functions, such as working memory and decision making, through innervation of specific regions of the telencephalon. In the zebrafish brain, most DA neurons innervating the telencephalon have their cell bodies located within the telencephalon itself (TelDA cells) (Tay et al., 2011; Yamamoto et al., 2011). To the best of our knowledge, there is no evidence for a plasticity of the neurotransmitter phenotype in these cells.

To perturb ENE in conditions close to physiological exposure and ecotoxicology, we used pharmacological treatments by balneation from 48 to 72 hours post fertilization (hpf). We then analyzed the consequences of these transient pharmacological treatments a few days later, between 6 and 7 dpf. We report quantifiable changes in the specification of the dopaminergic phenotype in TelDA neurons. We also report changes for high-speed swimming episodes. These results suggest a role of ENE on the specification of the dopaminergic phenotype and motor control in the zebrafish. They also open important perspectives for this model to decipher the chain of events leading from environmental factors to the pathogenesis of disorders such as schizophrenia and ADHD.

Materials and Methods

Fish strains

All experiments were carried out in accordance with animal care guidelines provided by the French ethical committee and under the supervision of authorized investigators.

Zebrafish were raised according to standards procedures. Briefly, for breeding, males and females zebrafish were placed overnight, in different compartments of a tank with a grid at the bottom that allows the eggs to fall through. The next morning the separation was removed and after few minutes, the eggs were collected, rinsed and placed in a petri dish containing embryo medium (EM). Embryos were kept at 28 degrees, then staged as hours post fertilization according to specific criteria. The number of animal used for each experiments is indicated in the corresponding figure legends.

Pharmacological treatments

Pharmacological compound, veratridine (10 µM), TTX (2 µM), ω conotoxin (0.08 µM), nifedipine (0.4 µM) and flunarizine (2 µM) were purchased form R&D System (UK) and prepared in water except veratridine which required dimethyl sulfoxide (DMSO) for dissolution and flunarizine that requires ethanol for dissolution. Sham control were performed using the same concentration of DMSO in EM without the drug to rule out an effect of the detergent itself. Specific period and duration of applications are indicated in the corresponding figure legends. All pharmacological treatments were performed by balneation followed by three washes in EM. Embryos were randomly distributed in wells (30 embryos per well) of a 6-well plate containing 5 mL of solution (EM+DMSO or EM+drug). Embryos exposed to drugs or the sham control solution were observed for morphological abnormalities every day until 5 dpf.

Malformations (*e.g*. spinal curvature, cardiac edema) were considered as experimental end-points and when detected the corresponding animals were excluded from the study.

Calcium imaging

At 24 hpf embryos of the (Hsp70:GAl4 x UAS:GCaMP6f;cry:mCherry) line were exposed to a 38°C temperature for 1.5 hour. Upon heat shock activation, GCamp6f is expressed in all the cells of the animals.

At 2-3 dpf the embryos were then individually embedded in low melting agarose, ventral side up for imaging.

30 min time lapse series were acquired at 1 Hz, at a single focal plane, on an Olympus BX60 microscope (Olympus corporation, Tokyo, Japan) equipped with a 40x 0.6N water immersion objective. A non-laser spinning disk system (DSD2, ANDOR Technology, Oxford, UK) was used for illumination and image acquisition. Images were open in Fiji and analyzed using Multi Measure (W. Rasband, B. Dougherty), Measure Stack (Optinav, Redmond, WA), and custom Image J plugins. Regions of interest (ROIs) were drawn manually over individual cell bodies. Movements of the preparation in the X/Y axis were corrected using the plugin Measure Stack. Average gray level from pixels in ROIs was measured over time. Spikes were defined as increase of fluorescence higher than 2 times the standard deviation of the baseline. The duration of spikes was calculated as the width at half-maximum. Incidence was scored as the number of cells generating transients divided by the estimated total number of cells in the imaged field and was expressed as a percentage. Frequency was calculated as the total number of transients in a given cell divided by the total acquisition time and was expressed as spikes per hour.

Immunohistochemistry

Tissue preparations

6-7 dpf zebrafish larvæ were deeply anesthetized using 0.2% Ethyl3-amniobenzoate methanesulfonate (MS222; Sigma-Aldrich) diluted in EM, then they were fixed in ice-cold 4% paraformaldehyde (PFA; Electron Microscopy Sciences) in 1X phosphate-buffered saline (PBS; Fisher Scientific) containing 0.1% Tween 20 % (PBST) overnight at 4 °C. Samples were dehydrated and stored in MeOH at -20°C.

Immunofluorescence

Immunofluorescence was performed in 2 mL microtubes. Unless specified otherwise in the protocol, incubations were performed at room temperature (RT), and thorough PBST washes were performed between each steps. The samples were first incubated in 3% Hydrogen Peroxide Solution (H_2O_2) in Ethanol 100% (EtOH) for 30 minutes, to deactivate endogenous peroxidases. They were then successively incubated in EtOH:Xylen 1:1 without agitation for 1 hour and, at -20 °C, in EtOH:Aceton 1:2 without agitation for 20 minutes. The washes were performed between these steps were performed in EtOH. After the final wash, samples were rehydrated in PBST.

In order to unmask the antigens, samples were incubated in PBST:Tris 150 mM pH9 for 10 minutes, then in Tris 150 mM pH9 at RT for 10 minutes and at 70 °C for 30 minutes. After PBST washes, the samples were incubated in a blocking buffer (10% normal goat serum (NGS), 1% triton X-100, 1% tween-20, 1% DMSO, 1% Bovin Serum Albumin (BSA) in PBS 1X) for 3 hours.

Two protocols were used for primary antibody staining. For the TH antibody, the samples were incubated with the first primary antibody (mouse anti-TH, 1:250) in a staining solution (1% NGS, 1% triton X-100, 1% DMSO, 1% BSA, 0,05% azide sodium

in PBST) at 4°C for 7-10 days, under gentle agitation. The samples were then incubated in a blocking buffer DAB (4% NGS, 0,3% triton X-100, 0,5% DMSO in PBST) for 1 hour at RT and incubated with a first secondary antibody (anti-mouse biotinylated, 1:200) in a secondary staining buffer (4%NGS, 0,1% triton X-100 in PBST) for 2,5 days at 4°C under gentle agitation.

For the revelation, we used the Vectastain ABC kit (Vector ®).Briefly, a AB mix was prepare by adding 10 µl of solution A and 10 µl of solution B in 1mL PBST/1% Triton-X100. One hour after the preparation, the samples were incubated in the AB mix for 1 hour. Samples were then incubated in Tyramid-TAMRA (1:200 in PBST) for 20 minutes, then 0,012% H_2O_2 was added directly in the solution and the samples were incubated for an additional 50 minutes.

Before a second primary antibody incubation, the samples underwent a step of fixation in PFA 4% for 2 hours at RT and washed overnight in PBST.

For the other primary antibodies (rabbit anti-caspase3, 1:500 or chicken anti-GFP, 1:500), the samples were incubated in the blocking buffer (1 hour when following a TH staining, 3 hours otherwise), then they were incubated with the primary antibody in a staining solution at 4 °C for 3-4 days, under gentle agitation. After washes, the samples were incubated with the second secondary antibody (goat anti-chicken Alexa Fluor 488, 1:500) and DAPI 1X in PBST at 4 °C for 2,5 days under gentle agitation. Samples were then washed three times in PBST and left overnight in PBST. For observation, the brain were dissected and mounted between slides and coverslides in Vectashield solution (Vector®).

Image acquisition

A Leica TCS SP8 laser scanning confocal microscope with a Leica HCTL Apo × 40/1.1 w objective was used to image the specimens.

Fluorescence signal was detected through laser excitation of fluorophores at 405, 488, 552, or 638 nm and detection was performed by two internal photomultipliers. Steps in the Z-axis were fixed at 1 µm. Acquired images were adjusted for brightness and contrast using ImageJ/FIJI software.

Quantification of immuno-reactive cells

The TH- and GFP-IR cells were counted manually from z-stacks of confocal images using the ImageJ cell counter plugin.

Spontaneous locomotion assays

Individual larvæ were placed in a well of a 24 well plate with 2 mL EM 2 hours before recordings for habituation. The plate is then placed in a Zebrabox (Viewpoint, Lyon, France) for 10 minutes recording sessions. Locomotor activity was recorded using ZebraLab software (Videotrack; ViewPoint Life Sciences, France). After a first session without threshold for 24 untreated larvæ the average speed (av_sp) of the batch was extracted from the data. For subsequent sessions, two threshold were applied. Swim bouts with a speed below half the average speed (av_sp/2) were considered as inactivity, episodes with a speed over twice the average speed (av_sp*2) were considered as fast episode or burst and episodes with a speed between the two threshold were considered as cruises episodes or normal swim.

For each sessions, each animal and each category of episodes (inactivity, cruises epiosdes and bursts episodes), 4 parameters are extracted from the recordings: the

number of episodes, the total distance covered, the duration of activity, and the average speed.

Experimental design

Statistical analyses

Results are shown as means ± SEM. Means comparisons were performed using the appropriate non parametric statistical tests (ANVOA, Mann Whitney U test or Kruskal-Wallis test depending on the experimental conditions). $P < 0.05$ was considered statistically significant and noted as follow: $P < 0.05$ (*), $P < 0.01$ (**), $P < 0.001$ (***).

For percentages, we used the 95% confidence interval defined as =1.96*squareroot((x*(1-x)/n)), n being the number of independent samples and x being the % of change observed.

All statistical tests were performed using the online software Brightstat and R.

Results

Presence of calcium spikes in the brain of zebrafish embryo.

To study Embryonic Neuronal Excitability (ENE) in the embryonic zebrafish brain, we recorded calcium spikes as a proxy. To follow the dynamics of intracellular calcium concentration we used the (Hsp70:GAl4 x UAS:GCaMP6f;cry:mCherry) transgenic line, in which the genetically encoded calcium reporter GCamp is expressed upon heat shock activation (see Materials and Methods). To monitor changes in fluorescence over time, we performed time-lapse imaging of the anterior most part of the brain of 2-3 dpf zebrafish embryos for 30 minutes sessions.

Spontaneous changes in fluorescence were detected in forebrain cells, likely including presumptive dopaminergic cells in the telencephalon and the OB (Figure 1A). We analyzed the evolution of the fluorescence from selected regions of interest corresponding to individual cell bodies (Figure 1B and Materials and methods). The average frequency of the recorded Ca^{2+} spikes was 6.6+/-5.4 spikes.h-1; the average incidence of these events was 45.2+/-9.7%; these events had a mean duration of 3.3/+- 1.6 s (n= 28 spikes from 5 independent preparations Figure 1C, blue boxplots). These parameters are in the range of what has been reported in the zebrafish spinal cord, confirming that the duration of Ca^{2+} spikes is shorter in zebrafish than in xenopus (Dulcis & Spitzer, 2008; Warp et al., 2012; Plazas et al., 2013).

Global pharmacological modifications of calcium spikes dynamics

In order to assess the effects of global manipulations of ENE, we applied pharmacological compounds directly in the embryo medium. The treatments were performed during the last day of embryonic development (48-72 hpf) to reduce the effects on early developmental steps such as neurulation and proliferation. These drugs were already used in *Xenopus* for similar purposes (Borodinsky et al., 2004). To increase calcium spiking we used veratridine (10 µM), which blocks the inactivation of voltage-dependent sodium channels. To decrease calcium spiking, we used a cocktail containing TTX (2 µM), ω-Conotoxin (0.08 µM), Nifedipine (0.4 µM) and Flunarizine (2 µM) targeting respectively voltage-dependent sodium channels; N, L and T subtypes of voltage dependent calcium channels (we refer to this cocktail as TCNF based on the initials of its 4 components).

We performed time-lapse recordings of the (Hsp70:GAl4 x UAS:GCaMP6f;cry:mCherry) transgenic line two to ten hours after the beginning of the treatments.

Following either veratridine treatment (n=26 spikes from 4 independent preparations) or TCNF treatment (n=15 from 4 independent preparations), individual events had a similar duration as in control (Kruskal-Wallis test, p=0.538; Figure 1C). Following veratridine treatments, the average frequency of calcium spikes was increased (+39.3+/-16%, n=36 cells from 4 independent preparations, p=0.206 bonferroni post-hoc test) as well as the average incidence of calcium transients (29.9+/-45% n=4 independent preparations, p<0.05 conover posthoc comparisons; Figure 1C, green boxplots).

Following TCNF treatments, the average frequency of calcium spikes was decreased (-29+/-22%, n=17 cells from 4 independent preparations, p=0.812 bonferroni post-hoc test) as well as the average incidence (-44+-/48% n=4 independent preparations, p<0.01 Kruskal-Wallis paired comparisons)(Figure 1C, red boxplots).

These results demonstrate that balneation treatments are able to change the incidence and frequency of spontaneous calcium spikes in the embryonic zebrafish forebrain. Based on these results, we refer to veratridine treatment as “increase of ENE”, and to TCNF treatment as “decrease of ENE”, in the following sections of the manuscript.

Dopaminergic cells in the telencephalon and the olfactory bulb (OB) in the zebrafish brain at larval stages.

To identify dopaminergic neurons in the telencephalon and the OB, we used two markers of the catecholaminergic phenotype, immune-labeled tyrosine hydroxylase 1 (TH1), the rate limiting enzyme for dopamine synthesis and the vesicular monoamines transporter (vMAT2) combined to anatomical landmarks such as the position of brain

ventricles or large fibers bundles. Indeed, in zebrafish, like in mammals, noradrenaline-containing neuronal soma are not detected in the forebrain anterior to the midbrain-hindbrain boundary, rather, they are restricted to neuronal subpopulations located in the nucleus locus coeruleus, the medulla oblongata and the area postrema (Ma, 1994a; b, 1997, 2003). Thus, all the catecholaminergic neurons located in front of the midbrain-hindbrain boundary are likely to be dopamine neurons.

To localize these markers we performed double wholemount immunohistochemistry on 6-7 dpf larvæ of the Tg(Et.vMAT2:eGFP) transgenic line. We used an anti-GFP antibody to amplify the endogenous GFP signal to visualize cells expressing vMAT2 (referred to as vMAT2+ cells in the remaining of the manuscript) and an anti-TH antibody to identify TH1 cells (referred to as TH1+ cells in the remaining of the manuscript). This anti-TH antibody is specific to TH1 and does not have affinity for TH2 (Yamamoto et al., 2011).

In control conditions, in the telencephalon, we detected 15.1+/-3.1 TH1+ cells (n= 39 samples from 6 independent experiments; Figure 2A, left column, Figure 2B, blue boxplot). The cell bodies of these neurons were distributed bilaterally along the midline, and relatively close to it. The major pattern of fibers distribution we could detect was that of fibers projecting first ventrally and then laterally joining the wide dopaminergic lateral longitudinal tracts.

An average of 63.4+/-6.7 vMAT2+ cells was also detected in this region (n= 39 samples from 6 independent experiments; Figure 2A, blue boxed column, Figure 2 C blue boxplot). The overall disposition of the cell bodies and projections was the same as for TH+ cells.

In control conditions, in the OB, 46.4+/-8.1 vMAT2+ cells and 30+/-2.6 TH1+ cells were detected (n= 39 samples from 6 independent experiments; Figure 2A, blue boxed column and Figure 2D and 2E, blue boxplot). The cell bodies of these OB TH1+ neurons were distributed at the anterior end of the forebrain and they were initially projecting in an anterior direction before rapidly branching in multiple directions.

In both regions, all TH1+ cells were also vMAT2+ while some vMAT2+ cells were TH1-. In the telencephalon, vMAT2+/TH1- cell bodies were mostly located at the anterior end of the cluster of vMAT2/TH1+ cells. Such $vMAT2^{+}/TH^{-}$ cells are also detected in the telencephalon of adult zebrafish (Yamamoto et al., 2011). Thus, in the developing zebrafish telencephalon, the population of $vMAT2^{+}$ cells slightly exceeds that of TH1-expressing cells.

Effects of pharmacological treatments on the expression of dopaminergic markers in the telencephalon and the OB.

To assess the effects of ENE on the expression of telencephalic dopaminergic markers at larval stages, we applied pharmacological treatments by balneation from 48 to 72 hpf as described above and performed whole-mount immunohistochemistry on larvæ fixed at 6-7 dpf.

Increasing the excitability in the zebrafish brain also increased the number of TH1+ cells both in the telencephalon and in the OB (+28.6+/-15%, $p<0.05$ and +45.9+/-17% $p<0.001$ respectively, n=35 samples from 6 independent experiments, conover posthoc comparisons, Figure 2A, green boxed column; Figure 2B and 2D, green boxplots). Meanwhile, the number of vMAT2 cells did not change significantly in either regions ($p=0.08$ for the telencephalon, $p=0.659$ for the OB, Kruskal wallis test; n=16 samples from 6 independent experiments; Figure 2A, green boxed column, Figure 2C,E, green boxplots).

Following decreased excitability, the number of TH1+ cells diminished in the telencephalon but not in the OB (-14.5+/-9.6% and -0.7+/-7.3% respectively, n=49 samples from 6 independent experiments; $p<0.001$ and $p>0.05$ respectively, conover posthoc comparisons, Figure 2A, red boxed column, Figure 2B and 2D, red boxplot). Meanwhile, the number of vMAT2 cells did not change significantly in either regions (Kruskal wallis test: $p=0.08$ for the OB, $p=0.659$ for the OB; n=24 from 6 independent experiments; Figure 2A, red boxed column and Figure 2C and 2E, red boxplots). In both experimental situations, that is, after increasing or decreasing ENE, all the TH1+ cells also exhibited vMAT2 labelling. Hence, according to our identification criteria (anatomical position combined to the expression of TH and vMAT2), an increase of embryonic electrical activity increases the number of TelDA cells, while a decrease of embryonic electrical activity decreases the number of TelDA cells.

On the other hand, the number of vMAT2+ cells was relatively stable in comparison to TH1+ cells following the perturbation of activity (only decreasing in the telencephalon following a decrease of activity). The stability of the number of vMAT2+ cells and the lower proportion of $vMAT2^{+}/TH^{-}$ cells following increase of ENE suggest that the cells that express a complete dopaminergic phenotype in this condition are recruited among a population of $vMAT2^{+}/TH^{-}$ cells. Hence $vMAT2^{+}/TH^{-}$ cells would behave as a reserve pool for dopaminergic cells (Dulcis & Spitzer, 2012). A similar conclusion could also apply to the OB, despite the fact that the number of TH1+ cells is not statistically diminished following decreased activity in this region. This unexpected result could account for a number of TH1+ cells already set at a minimum in basal conditions in the OB.

Modifications of ENE do not have an effect on cell death in the forebrain

To check whether increase or decrease of ENE could change cell survival, we

counted the number of cells IR for the apoptosis marker caspase-3 at 6-7 dpf. The number of caspase-3+ cells was stable following the increase or the decrease of ENE, strengthening the hypothesis that the changes observed in the number of TH1+ cells is indeed linked to changes in specification rather than changes in cell death (Figure 3).

Maturation of spontaneous swimming in zebrafish larvæ

In order to analyze the consequence of changes in ENE on motor behaviors in zebrafish larvæ, we recorded swimming episodes, as described in Materials and Methods. During locomotion, zebrafish larvæ display successive turn and swim bouts called episodes, interleaved with resting periods. This behavior can be analyzed by semi-automated methods, making possible to distinguish between episodes based on the average swim speed. Swimming episodes with a speed close to the overall average speed of all recorded episodes are considered as cruises episodes or normal swim. Episodes with a speed higher than twice the overall average speed of all recorded swim episodes, are considered as fast episodes or bursts.

We first studied the dynamic of maturation of larval cruises and bursts episodes in control conditions. We tracked the position of individual larvæ during 3 rounds of 10 minutes recordings at 4, 5, 6 and 7 dpf. The recorded parameters reflected a gradual increase of spontaneous locomotion from 4 to 6 dpf and a relative stability between 6 and 7dpf. From 4 to 6 dpf, the number of episodes, the duration of swimming and distance covered increases, both for cruises and bursts episodes ($p<0.01$ for each parameters, Bonferroni post-hoc test, n=48 individuals for each stages; Figure 4, lighter blue boxplots). In contrast, between 6 and 7 dpf, the recorded parameters were stable both for cruises and bursts episodes ($p=0.16$, 1 and 1 respectively; Figure 4, darker blue boxplots). Based on these results, we concluded that we could set our analysis window between 6 and 7 dpf.

Effects of pharmacological treatments on the locomotion of 6-7 dpf larvæ.

We next studied the effect of transient increase and decrease of ENE during the embryonic period on locomotion recorded in larval zebrafish (Figure 5A). We recorded spontaneous locomotion of 6-7 dpf zebrafish larvæ over 3 consecutive 10 minutes sessions in 3 conditions: control, increased ENE, and decreased ENE. A representative example of traces obtained for 24 well plates for each conditions is shown in Figure 5B. For cruises and bursts episodes, the four parameters measured were the number of swim bouts, the total duration of swim, the total distance covered, the average speed of swim (Figure 5 C-J).

For cruises episodes, in control conditions, the four measured parameters were the number of swim bouts: 1267.2+/-292.3, total duration: 306.5+/-58.6 s, total distance covered: 767.5+/-285.1 mm and average speed: 2.5+/-0.7 $mm.s^{-1}$ (n=318 larvæ from 15 independent experiments, Figure 5B-F, blue boxplots).

The number of swim bouts was decreased following both the increase and the decrease of ENE (-5.8+/-2.3% ; -22+/-5% respectively, Figure 5C). The three other parameters increased either after an increase or a decrease of ENE (the total duration: +4.6+/-2.1% ; +35.4+/-5.8%; the total distance covered: +38.3+/-4.9% ; +14.7+/-4.3% and average speed: +34,6+/-4.8% ; +22.2+/-5% respectively, $p<0.01$ conover posthoc comparisons; n>262 larvæ from 15 independent experiments; Figure 5D-F).

For bursts episodes, in control conditions, the 4 parameters studied were the number of swim bouts: 301+/-227.6, the total duration: 42+/-38.4 s, the total distance covered: 434.2+/-492.6 mm and the average speed of swim: 9.7+/-2.8 $mm.s^{-1}$ (Figure 5 G-J, blue boxplots).

Three of these parameters changed according to the treatments. They increased following an increase of ENE and decreased following a decrease of ENE (number of swim bouts: +24.6+/-4%;-54.8+/-6%; total duration: +37.8+/-4.8%;-58+/-6%; total distance covered: +58.8+/-5%;-61.6+/-5.9% respectively, % of change followed by the confidence interval, n>262 larvæ from 15 independent experiments; p<0.01 conover posthoc comparisons, Figure 5G-J). Average speed also increased following a increase of ENE (+17+/-3.8% Figure 5J, green boxplot) while it did not change following a decrease of ENE (Figure 5J, red boxplot).

These results showed that the consequences of perturbing the embryonic electrical excitability are different on the cruises episodes and on bursts episodes, suggesting that the underlying neural networks of these swimming modes are not the same and/or that they are not regulated in the same way following changes in ENE.

Kinetics of the direct effects of acute pharmacological treatments on the locomotion of 6-7 dpf larvæ.

To exclude a direct effect of the drugs used on the larvæ locomotion, we next followed the time course of the effects of acute pharmacological treatments (veratridine and TCNF) in 6-7 dpf larvæ. We performed 10 minutes recording sessions before application of the treatments, then +2 hours, and 24 hours after the treatments.

For cruises episodes, the results obtained following acute veratridine applications are close from the one induced by the embryonic applications with a decrease of the number of episodes and an increase of the duration and the distance. Only the results for the average speed are different since it was not significantly different following acute application while it increased following embryonic application (Figure 6A-D green boxplots). Following T.C.N.F applications the number of events decreased like similarly

as following embryonic application while duration, distance and average speed remained unchanged (Figure 6A-D red boxplots).

For bursts episodes, acute treatments had overall similar effects on the recorded parameters as the one recorded after treatments performed in 2-3 dpf embryos (Figure 6). Veratridine application induced an increase of duration and distance, while the number of events and the average speed were not significantly different (Figure 6E-H green boxplots). T.C.N.F application led to a decrease of number of events, duration and distance during bursts, only the average speed remained unchanged (Figure 6E- H red boxplots).

By the next day, while some of the effects of the acute treatments are still detectable, all the effects of these treatments on bursts episodes had faded away (Figure 6E-H, lighter colored boxplots). These results clearly show that the delay between the embryonic treatments and our analysis of larval locomotion is longer than the time required for the disappearance of the acute effect of the drugs. Hence, these results support the existence of a long-term effect related to changes in electrical activity during the embryonic period in the zebrafish.

Discussion (1261 / 1500w)

Summary

Immature forms of excitability, referred to here as Embryonic Neuronal Excitability (ENE), including calcium spikes and activation of non-synaptic receptors to neurotransmitters, contribute to modulate neuronal differentiation. Here we show that the developing zebrafish is a suitable model to manipulate ENE using pharmacological treatments and to study the consequences of these manipulations on the plasticity of neuromodulator systems, at works in the pathogenesis of several human neuropsychiatric diseases. Indeed, we report that ENE exerts a positive regulatory effect on the specification of the dopaminergic phenotype by increasing the number of dopamine cells in the telencephalon. The pharmacological manipulation of ENE has also a clear behavioral outcome by changing the occurrence of high-speed episodes of swimming in zebrafish larvæ.

Balneation treatments and ENE

For the present study, zebrafish embryos were exposed to pharmacological compounds by means of balneation treatments. This methodological approach allows performing global and transient drugs applications, relevant to natural situations where embryos can be exposed to various biologically active or toxic compounds. Zebrafish is highly suitable for such questions because of its external development in an egg, and because its blood brain barrier is not fully mature until 10 dpf, allowing diffusion of the drugs to the neuronal tissues. As a consequence, we were able to analyze alterations by pharmacological treatments of calcium transients, one of the main form of immature excitability.

We focused on calcium transients to assess the effectiveness of the treatments, but other intercellular communication processes such as the paracrine activation of GABA

and glutamate receptors by endogenous transmitters are also likely perturbed by the treatments. Further studies are required to decipher the specific contribution of each of these mechanisms to the cellular and behavioral effects we reported here.

Calcium transients in the zebrafish forebrain

One reason to focus on calcium transients is that they have been involved in neurotransmitter phenotype specification in other models of neuronal plasticity. In addition, calcium transients are conveniently measured by calcium imaging.

Calcium transients were already reported in the spinal cord of zebrafish embryos around 24 hpf. Here, recordings were performed in the forebrain of embryonic zebrafish around 48 hpf, a time at which the transition toward synaptic network activity has occurred in the spinal cord. These observations are in accordance with the existence of an postero-anterior gradient of neuronal maturation, similar to what was described in xenopus.

Calcium transients in the forebrain had frequency and duration similar to what has been described in the zebrafish spinal cord. This duration is overall shorter than what has been observed in the Xenopus nervous system. The basis of these interspecies differences are not known, but it suggests that the duration of the transients is not necessarily the pertinent signal to trigger the effect on neuronal differentiation. This is further suggested by the results of the TCNF treatments reported here, which lead to changes in DA specification and in locomotion parameters, while the duration of individual spikes duration was not changed.

We chose to drive the expression of GCamp by an exogenous trigger, here a heat-shock. This allowed the expression of the calcium reporter in all the cells present at the selected period of recordings. The next step of our approach will thus be to use differentiation markers of the DA lineage to identify the differentiation status of the cells

where the Ca^{2+} spikes are detected, and also to see whether there are different dynamics of the calcium transients between different subregions of interest in the embryonic brain by using whole brain calcium imaging.

Identification of a biomarker for DA reserve pool neurons?

The effect of ENE perturbations on the DA phenotype analyzed by the number of TH1+ cells was in agreement with the homeostatic rule described in xenopus. Indeed, DA phenotype was enhanced by increased excitability, as expected from an overall inhibitory neurotransmitter. The relative constancy of the number of vMAT2+ cells, together with the absence of significant change is caspase 3-labelled cells upon treatments, suggest that modulation of excitability did not affect cell death or proliferation, but rather triggered a plasticity of the dopaminergic phenotype. This plasticity of the DA phenotype is likely to occur within the pool of vMAT2+ cells, since the number of VMAT2+/TH+ was increased with increased excitability, at the expense of VMAT2+/TH- cells. Therefore, the VMAT2+/TH- cells would be a reserve pool of cells primed to become dopamine neurons when plasticity-triggering events occur. Although somewhat peculiar at first sight, the expression of the vesicular transporter in a reserve pools of cells, might have a functional advantage in term of response to plasticity-triggering events, limiting the number of factors to be changed for reaching a fully functional dopamine phenotype.

Behavioral consequences of ENE

Perturbations of ENE had also behavioral consequences in zebrafish larvæ. For bursts episodes, the initiation of movement is likely to be the prime parameter modified following ENE perturbations. Interestingly, hyperlocomotion is an endophenotype related to ADHD and schizophrenia in zebrafish (Blin et al., 2008; Lange et al., 2018). Determining whether a direct activation of TelDA cells could trigger an increase of

543 bursts episodes is an interesting perspective for the future, as seeing whether other
544 behaviors related to ADHD and schizophrenia such as prepulse inhibition are also
545 affected by alterations of ENE.

546 *Critical period for the effect of ENE perturbations*

547 We observed an effect of the pharmacological treatments performed during the
548 embryonic period on spontaneous locomotion several days after the end of the
549 treatments. In contrast, no effects were observed 24 hours after treatments performed
550 at 6 dpf in the zebrafish larvæ. These long-lasting effects of treatments at specific
551 embryonic time are in line with the existence of a critical developmental period, more
552 sensitive to homeostatic perturbations, promoting therefore significant phenotypic
553 plasticity in immature neurons. Interestingly, dopaminergic systems have multiple
554 functional role and are particularly prone to plasticity events, suggesting that these
555 systems might be a key factor for adaptability of the animals to environmental changes.
556 Whether it is a cause, a consequence or a simple correlation of their conservation
557 throughout animal evolution is still an open question.

558 *Potential involvement of changes of ENE in the pathogenesis of brain disease*

559 According to the 'Developmental Origins of Health and Disease (DOHaD)
560 hypothesis, transient exposure to perturbations during the development could lead to
561 emergence of disease in young or adult individuals (Mandy & Nyirenda, 2018).
562 Neurological and psychiatric diseases, such as autism spectrum disorders, ADHD, or
563 schizophrenia are hypothesized to have a developmental origin. The environmental
564 factors potentially contributing to these pathologies include malnutrition, stress, and
565 drugs exposure during the embryonic period.

566 Results from epidemiological studies and experiments in rodents further suggest
567 that a range of functional and behavioral abnormalities observed in the mature system

result from early alterations of dopaminergic neurons differentiation. The data presented here point to an implication of ENE in the regulation of dopaminergic differentiation in the developing brain, suggesting that ENE could act as an intermediate between environmental factors and the molecular changes leading to the alteration of dopamine-related behaviors.

These results provide a firm basis to dissect further the cellular and molecular mechanisms linking exposure to external challenges with the subsequent changes in ENE, in the maturation of the dopaminergic systems and its behavioral outputs. A comparative study of the transcription factors differentially expressed in vMAT2 cells following changes in ENE, would help identify dopaminergic related factors having an activity-dependent expression, including epigenetic effectors (level of methylation, histone acetylation).

Such mechanisms are underlying phenotypes related to ADHD and schizophrenia in zebrafish, and opens new avenues to better understand how environmental factors could promote developmental brain disorders such as schizophrenia and ADHD.

Bibliography

Blankenship AG & Feller MB (2010) Mechanisms underlying spontaneous patterned activity in developing neural circuits. Nat.Rev.Neurosci. 11:18–29.

Blin M, Norton W, Bally-Cuif L, Vernier P, Laure B-C & Vernier P (2008) NR4A2 controls the differentiation of selective dopaminergic nuclei in the zebrafish brain. Molecular and cellular neurosciences 39:592–604.

Borodinsky LN, Root CM, Cronin JA, Sann SB, Gu X & Spitzer NC (2004) Activity-dependent homeostatic specification of transmitter expression in embryonic neurons. Nature 429:523–530.

592 Crepel V, Aronov D, Jorquera I, Represa A, Ben-Ari Y & Cossart R (2007) A
593 parturition-associated nonsynaptic coherent activity pattern in the developing
594 hippocampus. Neuron 54:105–120.

595 Demarque M, Represa A, Becq H, Khalilov I, Ben-Ari Y & Aniksztejn L (2002)
596 Paracrine intercellular communication by a Ca2+- and SNARE-independent
597 release of GABA and glutamate prior to synapse formation. Neuron 36:1051–
598 1061.

599 Demarque M & Spitzer NC (2010) Activity-Dependent Expression of Lmx1b
600 Regulates Specification of Serotonergic Neurons Modulating Swimming
601 Behavior. Neuron 67:321–334.

602 Dulcis D, Jamshidi P, Leutgeb S & Spitzer NC (2013) Neurotransmitter switching in
603 the adult brain regulates behavior. Science 340:449–453.

604 Dulcis D, Lippi G, Stark CJ, Do LH, Berg DK & Spitzer NC (2017) Neurotransmitter
605 Switching Regulated by miRNAs Controls Changes in Social Preference. Neuron
606 95:1319-1333.e5.

607 Dulcis D & Spitzer NC (2008) Illumination controls differentiation of dopamine
608 neurons regulating behaviour. Nature 456:195–201.

609 Dulcis D & Spitzer NC (2012) Reserve pool neuron transmitter respecification: Novel
610 neuroplasticity. Developmental Neurobiology 72:465–474.

611 Gawel K, Banono NS, Michalak A & Esguerra C V. (2019) A critical review of
612 zebrafish schizophrenia models: Time for validation? Neuroscience and
613 Biobehavioral Reviews 107:6–22.

614 Gomez TM, Robles E, Poo M & Spitzer NC (2001) Filopodial calcium transients

615 promote substrate-dependent growth cone turning. Science 291:1983–1987.

616 Gomez TM & Spitzer NC (1999) In vivo regulation of axon extension and pathfinding
617 by growth-cone calcium transients. Nature 397:350–355.

618 Klein MO, Battagello DS, Cardoso AR, Hauser DN, Bittencourt JC & Correa RG
619 (2019) Dopamine: Functions, Signaling, and Association with Neurological
620 Diseases. Cellular and Molecular Neurobiology 39:31–59.

621 Lange M, Froc C, Grunwald H, Norton WHJ & Bally-Cuif L (2018) Pharmacological
622 analysis of zebrafish lphn3.1 morphant larvae suggests that saturated
623 dopaminergic signaling could underlie the ADHD-like locomotor hyperactivity.
624 Progress in Neuro-Psychopharmacology and Biological Psychiatry 84:181–189.

625 Lange M, Norton W, Coolen M, Chaminade M, Merker S, Proft F, Schmitt A, Vernier
626 P, Lesch K-P & Bally-Cuif L (2012) The ADHD-linked gene Lphn3.1 controls
627 locomotor activity and impulsivity in zebrafish. Molecular psychiatry 17:855.

628 Ma PM (1994a) Catecholaminergic systems in the zebrafish. I. Number, morphology,
629 and histochemical characteristics of neurons in the locus coeruleus. Journal of
630 Comparative Neurology 344:242–255.

631 Ma PM (1994b) Catecholaminergic systems in the zebrafish. II. Projection pathways
632 and pattern of termination of the locus coeruleus. Journal of Comparative
633 Neurology 344:256–269.

634 Ma PM (1997) Catecholaminergic systems in the zebrafish. III. Organization and
635 projection pattern of medullary dopaminergic and noradrenergic neurons.
636 Journal of Comparative Neurology 381:411–427.

637 Ma PM (2003) Catecholaminergic systems in the zebrafish. IV. Organization and

projection pattern of dopaminergic neurons in the diencephalon. Journal of Comparative Neurology 460:13–37.

Mandy M & Nyirenda M (2018) Developmental Origins of Health and Disease: the relevance to developing nations. International health 10:66–70.

Murray RM, Bhavsar V, Tripoli G & Howes O (2017) 30 Years on: How the Neurodevelopmental Hypothesis of Schizophrenia Morphed Into the Developmental Risk Factor Model of Psychosis. Schizophrenia Bulletin 43:1190–1196.

Owens DF & Kriegstein AR (1998) Patterns of intracellular calcium fluctuation in precursor cells of the neocortical ventricular zone. Journal of Neuroscience 18:5374–5388.

Owens DF & Kriegstein AR (2002) Is there more to GABA than synaptic inhibition? Nat.Rev.Neurosci. 3:715–727.

Plazas P V, Nicol N & Spitzer NC (2013) Activity-dependent competition regulates motor neuron axon pathfinding via PlexinA3. Proceedings of the National Academy of Sciences of the United States of America 110:1524–1529.

Scain AL, Le Corronc H, Allain AE, Muller E, Rigo JM, Meyrand P, Branchereau P & Legendre P (2010) Glycine release from radial cells modulates the spontaneous activity and its propagation during early spinal cord development. Journal of Neuroscience 30:390–403.

Schweitzer J & Driever W (2009) Development of the dopamine systems in zebrafish. Adv Exp Med Biol 651:1–14.

Schweitzer J, Löhr H, Filippi A & Driever W (2012) Dopaminergic and noradrenergic

661 circuit development in zebrafish. Developmental Neurobiology 72:256–268.

662 Spitzer NC, Kingston PA, Manning TJ & Conklin MW (2002) Outside and in:
663 development of neuronal excitability. Curr.Opin.Neurobiol. 12:315–323.

664 Tay TL, Ronneberger O, Ryu S, Nitschke R & Driever W (2011) Comprehensive
665 catecholaminergic projectome analysis reveals single-neuron integration of
666 zebrafish ascending and descending dopaminergic systems. Nature
667 Communications 2:112–171.

668 Warp E, Agarwal G, Wyart C, Friedmann D, Oldfield CS, Conner A, Del Bene F,
669 Arrenberg AB, Baier H, Isacoff EY, Bene F, Arrenberg AB, Baier H & Isacoff EY
670 (2012) Emergence of patterned activity in the developing zebrafish spinal cord.
671 Current Biology 22:93–102.

672 Yamamoto K, Ruuskanen JO, Wullimann MF & Vernier P (2011) Differential
673 expression of dopaminergic cell markers in the adult zebrafish forebrain. The
674 Journal of comparative neurology 519:576–598.

675

676

Figure legends

Figure 1 Presence of calcium spikes in the zebrafish telencephalon and their manipulations by transient balneation in pharmacological agents.

A. Consecutive images of a confocal time series of the brain of 48 hpf of Et(hsp:gal4;UAS:GCamp6f) embryos in control conditions. Fluorescence is displayed on a pseudocolor scale, the look up images intensity scale coding is shown in the right corner of the first image. Scale bar is 100µm. White dash circle surround the cell body of a cell displaying a calcium transient.

B. Changes in fluorescence intensity are plotted as a function of time. Ca2+ transients were scored for fluorescence changes, more than two times the SD of the baseline (dashed lines), and >3 sec in duration, calculated as the width at half-maximum. Representative traces from control conditions (in blue), following veratridine treatment (in green) and following treatment with a pharmacological cocktail containing TTX (2.5 µM), ω-Conotoxin (0.1 µM), Nifedipine (0.5 µM) and Flunarizine (2.5 µM) (TCNF, in red).

C. Left, boxplots showing the mean duration of single calcium spikes in control conditions (in blue, 3.3+/-1.6 sec), following veratridine treatment (in green, 3.7+/-1.7 sec) and following TCNF treatment (in red, 3.4+/-1.4 sec).

Middle, boxplots showing the mean frequency of calcium transients in control conditions (in blue, 6.6+/-5.4 spikes per hour, n=28 cells from 5 independent preparations), following veratridine treatment (in green, 9.2+/-6.6 spikes per hour, n=36 cells form 4 independent preparations) and following TCNF treatment (in red, 4.7+/-3 spikes per hour, n=17 cells form 4 independent preparations).

Right, boxplots showing the mean incidence of single calcium spikes in control conditions (in blue, 45.2+/-9.7%, n=5 independent preparations), following veratridine treatment (in green, 58.8+/-9.7%, n=4 independent preparations) and in the presence of TCNF (in red, 4.7+/-3 spikes per hour, n=17 cells form 4 independent preparations).

Figure 2 Effects of 24hrs balneation treatment on the number of dopaminergic neurons in the zebrafish larval telencephalon and OB.

A. Maximum projection of confocal z series of the brain of 6-7 dpf Et(VMAT2:eGFP) larvæ, in control conditions (left column boxed in blue), in the presence of veratridine (middle column, boxed in green) and in the presence of TCNF (right column, boxed in red). Immunostaining to TH (magenta) and GFP (cyan) and DAPI (yellow) are shown as merge and individual channels. Scale bars = 50 µm.

B-E. Boxplots showing the mean number of IR cells in control conditions, in the presence of veratridine and in the presence of “TCNF” in the telencephalon (B,C) and in the olfactory bulb (C,D), for TH (B,D) and for GFP (vMAT2 cells, C,E).

Figure 3 Absence of changes in cell death following increase or decrease of ENE

A. Maximum projection of confocal z series of the brain of 6-7 dpf Et(VMAT2:eGFP) larvæ, in control conditions (left image boxed in blue), in the presence of veratridine (middle image, boxed in green) and in the presence of TCNF (right image, boxed in red). Immunostaining to caspase-3 (magenta) and GFP (cyan) are shown as merged channels. Scale bars = 50 µm.

B. Boxplots showing the mean number of IR cells in control conditions, in the presence of veratridine and in the presence of “TCNF” for the caspase-3 staining in the olfactory bulb and the telencephalon.

Figure 4 Maturation of locomotion parameters

A-H. Boxplots showing the mean of 4 swimming parameters, number of episode (A,E), total duration (B,F), distance covered during swimming (C,G) and speed (D,H) for cruises episodes (A-D) and for bursts episodes (E-H) at different stage of larval development (4, 5, 6, and 7dpf).

Figure 5 Effects of 24hrs balneation treatments during embryonic development on spontaneous swimming of zebrafish larvæ.

A. Time line of the experiments indicating the timing (in days post fertilization, dpf) for the pharmacological treatments, and the following locomotion tests.

B. Representative path reconstructions for 24 individual larvæ during a 10 minutes trial for three experimental conditions. The portion of the path corresponding to bursts episodes (shown in red) are longer when early activity is increased (veratridine treatment) and shorter when early activity is decreased (T.C.N.F. treatment).

C-J. Boxplots showing the mean of different swimming parameters in different experimental conditions, Mean number of episode (C,G), total duration (D,H), distance covered during swimming (E,I) and speed (F,J) are shown for cruises episodes (C-F) and for bursts episodes (G-J).

Figure 6 Effects of 2hrs acute balneation treatments on zebrafish spontaneous swimming.

A-H. Boxplots showing the mean of different swimming parameters, mean number of episode (A,E), total duration (B,F), distance covered during swimming (C,G) and speed (D,H), for cruises episodes (A-D) and for bursts episodes (E-H), in different experimental conditions. The effects of 2hrs acute treatments with DMSO,

Veratridine, or TCNF are compared to pre-application recordings and 24hrs post-application recordings.

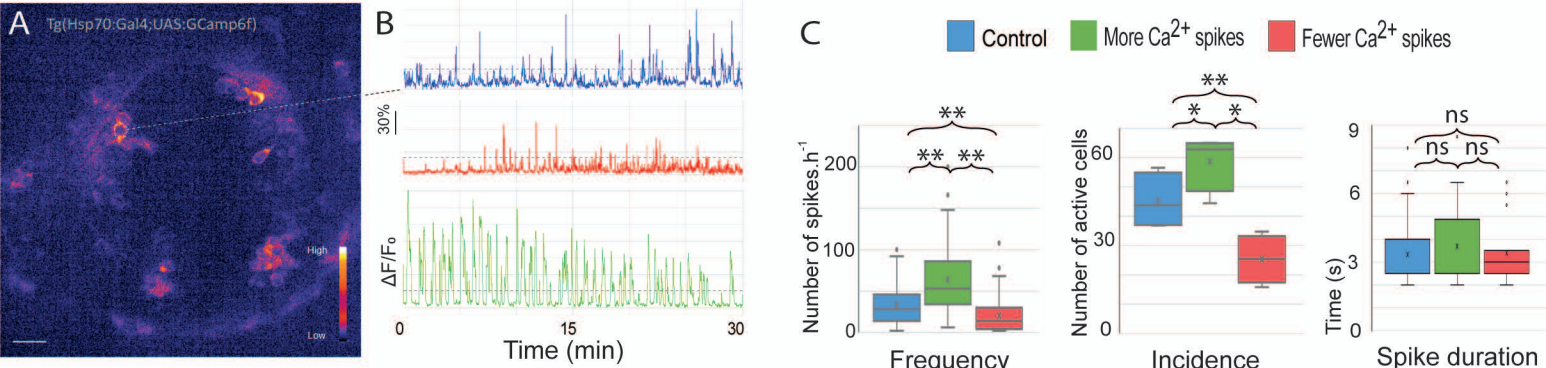

Bataille et al., Figure 1. Calcium spikes and their modulation by pharmacological treatments, in the embryonic zebrafish forebrain

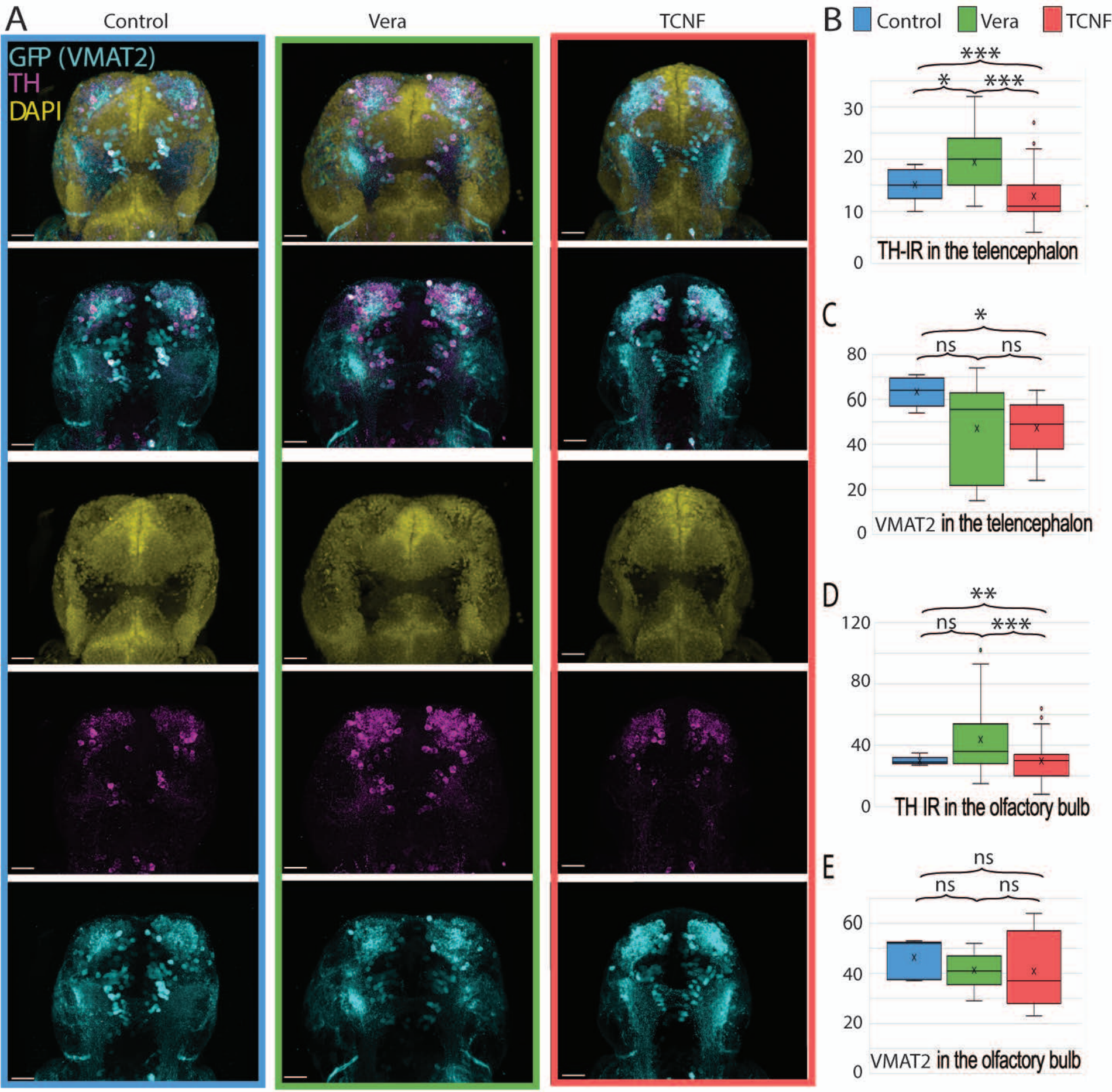

Bataille et al., Figure 2. Effects of ENE on the numbre of DA neurons in the zebrafish forebrain

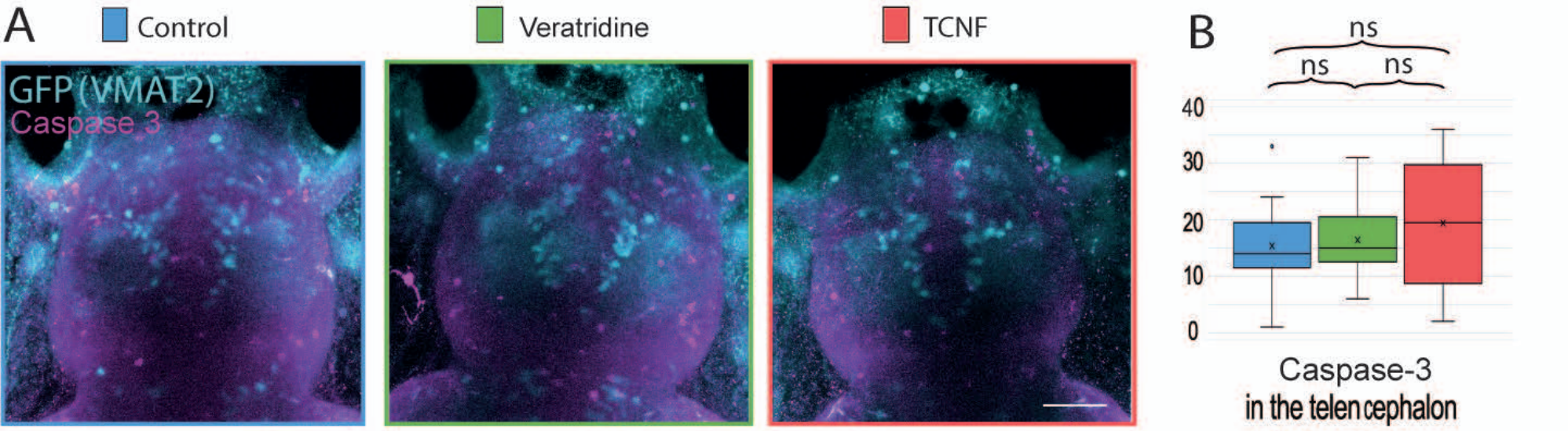

Bataille et al., Figure 3. Effects of ENE on caspase-3 expression in the larval zebrafish forebrain

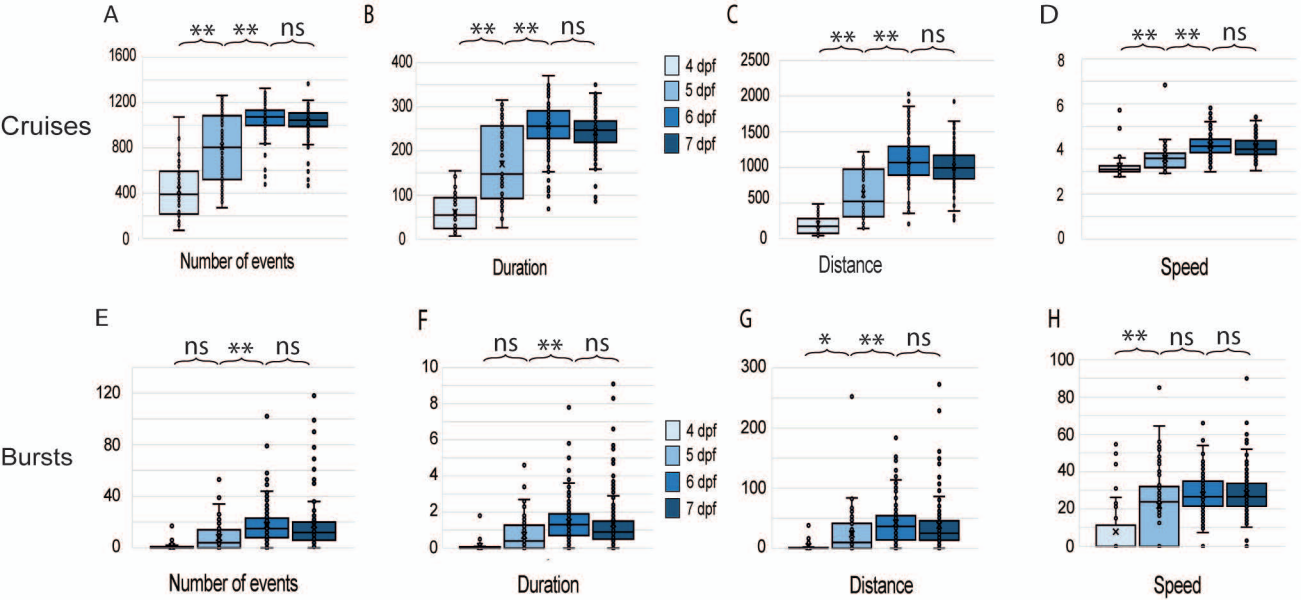

Bataille et al., Figure 4. Development of zebrafish spontaneous locomotion

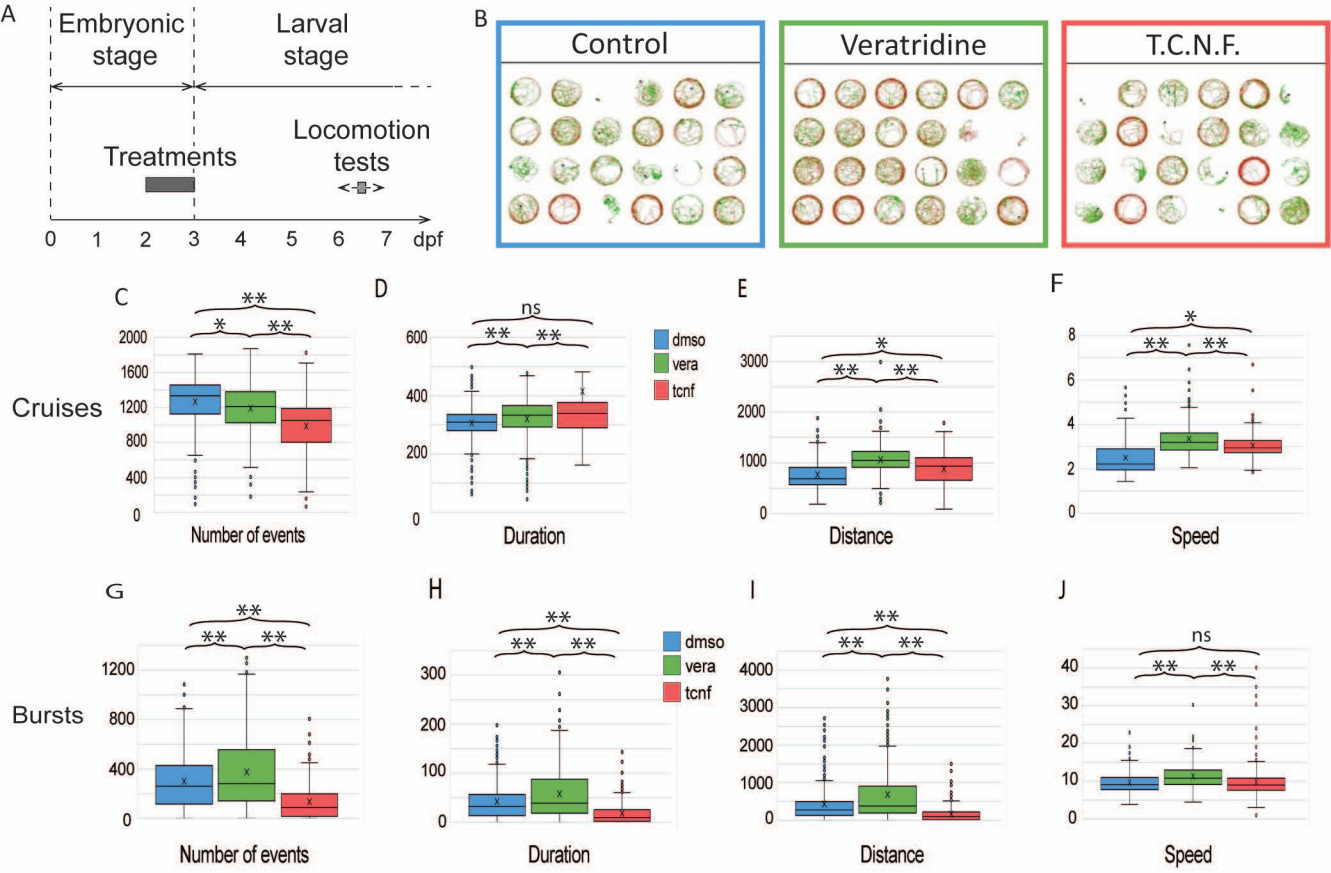

Bataille et al., Figure 5. Effects of ENE on the zebrafish spontaneous locomotion

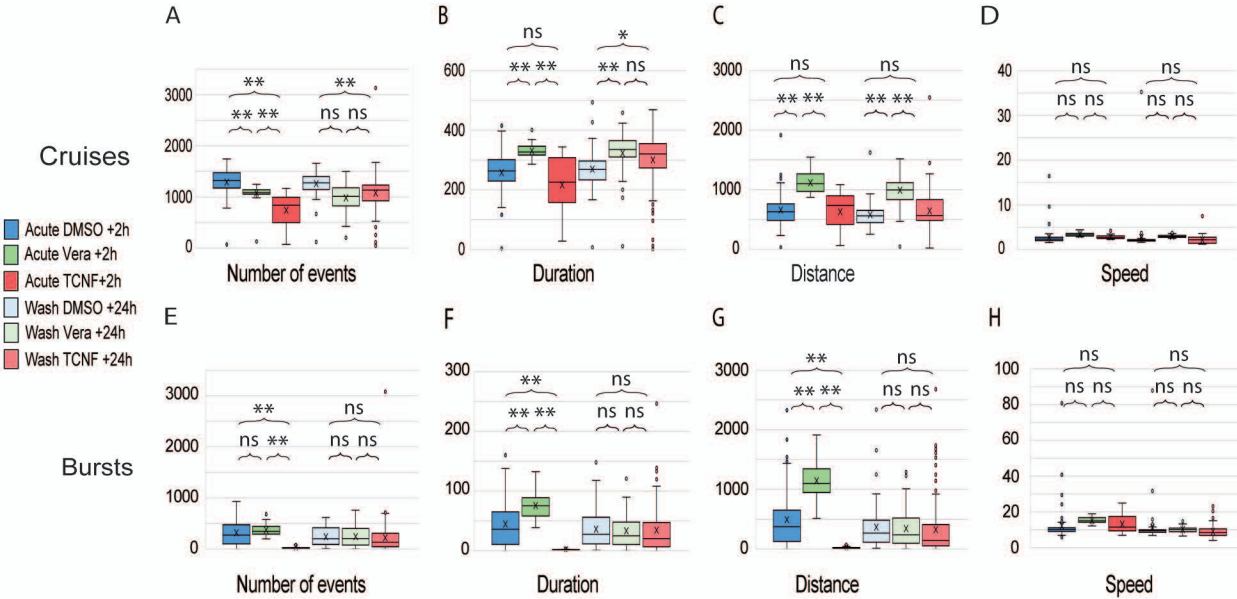

Bataille et al., Figure 6. Effects of acute pharmacological treatments on the zebrafish spontaneous locomotion